Research Article

Halil Berberoğlu*, Mehmet Tiken, Kemal Efe Eseller, Elif Orhan, and Can Candan

Performance evaluation of self-mixing interferometer with the ceramic type piezoelectric accelerometers

https://doi.org/10.1515/phys-2022-0011
received October 19, 2021; accepted January 19, 2022

Abstract: In this article, reconstructed displacement from the self-mixing signal is compared with the displacement obtained by the ceramic shear mode design piezoelectric accelerometer. Piezoelectric accelerometers are widely accepted due to the low output noise and wide frequency range, but nevertheless it is not contact-free. Self-mixing interferometric signals due to the vibrating target on which an accelerometer is attached are acquired by an external silicon type photodetector. The laser light hits directly the accelerometer as a target which is driven by the sum of two different sinusoidal frequencies of 150 and 300 Hz with different voltage levels.

Keywords: self-mixing laser diode, phase unwrapping, interferometry

1 Introduction

Self-mixing interferometry (SMI) has considerable impact in the area of optical metrological sensing with many interesting applications at the cost of minimal elementary optical setup [1,2]. The major observable parameters are the displacement, velocity, absolute distance, and vibration frequencies. The principles of self-mixing occurring in the laser cavity have been well understood and extensively studied in the literature [3–8]. Because of the high efficiency of light coupling out of the laser cavity of the semiconductor laser diodes, even in the case of weakly reflected light coming from the target, self-mixing effect is particularly strong due to its active gain medium and low reflection coefficients of lasing cavity. Reflected laser light couples back into the laser cavity where it interacts with the original laser light source. This causes a fluctuation in the laser power which can be detected by the photodetectors that is located on the opposite side of the laser cavity other than primary output. Semiconductor laser diode feedback was first modeled by Lang and Kobayashi [9] in 1980, where the electric fields are used to explain the modulation. This model explained only the weak to moderate optical feedback into the single mode laser diode. The dimensionless feedback parameter that depends on the amount of laser light reflected into the lasing cavity was introduced by this model as following [9].

$$C = \kappa \frac{\tau}{\tau_{\text{in}}} \sqrt{1 + \alpha^2}, \tag{1}$$

where κ is the coupling coefficient that depends on reflectivity of the exit laser facet and the reflectivity of the target, τ_{in} and τ are the internal and external cavity round trip time for the laser light, and α is the linewidth enhancement factor. The C parameter, depending on the level of feedback, is important in terms of understanding the different feedback regimes that the laser is operating. Due to the interaction between the target and laser light, the output power of laser light becomes modulated (P_{f}) which can be directly obtained by the Lang and Kobayashi equation,

$$P_{\text{f}} = P_0(1 + m\cos(2\pi\nu_{\text{f}}\tau)), \tag{2}$$

where m is the modulation index, P_0 is the optical power without feedback, and ν_{f} is the emitted frequency of the laser under the feedback.

In this study, we compared the performance of ceramic shear-based piezoelectric accelerometer with the obtained

* Corresponding author: Halil Berberoğlu, Physics Department, Ankara Haci Bayram Veli University, Polatli Faculty of Science and Letters, 06900 Polatli, Ankara, Turkey,
e-mail: halil.berberoglu@hbv.edu.tr
Mehmet Tiken: Avionic Department, 5th Main Maintenance Factory Directorate, Ankara, Turkey; Department of Advanced Technology, Gazi University, Graduate School of Natural and Applied Science, Ankara, Turkey
Kemal Efe Eseller: Department of Electrical – Electronics Engineering, Atilim University, Ankara, Turkey
Elif Orhan, Can Candan: Physics Department, Science Faculty, Gazi University, Ankara, Turkey

self-mixing interferometric signals as a result of vibrations of sum of two frequencies. In order to retrieve the real target movement, solid state accelerometers were used to compensate the undesirable vibrations which degrade the self-mixing signals [10]. The advantage of used accelerometer is its broadband resolution of 0.001 m/s^2 (RMS) in the range from 1 to 10 kHz. In the present work, construction of displacement was performed in the moderate feedback regime in which self-mixing was saw-tooth like interferometric signal.

Basic resolution of displacement for SMI is half of the wavelength of the laser. However, phase unwrapping method (PUM) was often used to improve the resolution much better than half wavelength of the laser [11,12]. Proposed by Zabit *et al.* [12], adaptive transition detection algorithm based on phase unwrapped differentiates from weak to strong self-mixing regimes and automatically detects the optimized threshold level so that it can detect all self-mixing signals independent from the feedback. The standard procedure for phase unwrapping has been used that is explained in Section 2.

Previous similar SMI setups are listed in Table 1 [10–13]. We have used the ceramic type sensing element of accelerometers which has a resolution of 0.0001*g* (RMS) (where *g* is the acceleration of gravity) over very broad range from 1 to 10 kHz for the first time. Also, Si photodetector has been used in our system which is more advanced than built-in detector in the laser. Besides, spectral noise performance of ceramic accelerometer is better than most of the solid state type accelerometers and it is given as 3 $\mu g/\sqrt{Hz}$ at 100 Hz which corresponds to approximately 15 nm (cut-off frequency used in this calculation is 500 Hz) based on the calculation used by Zabit *et al.* [10], which is in the limit of our sensing capability of self-mixing experiment. Moreover, in our work, the calibration of accelerometer was checked by the calibration exciter (Type 4294, Brüel&Kjaer) that drives the accelerometer. Also, we have used a shaker which is not a simple one and it is driven by the NI module, and acquired signal is synchronized with the driven shaker. When we consider all of these, our instrumentation has been used with ceramic shear type sensor in this self-mixing study for the first time.

2 Experimental method

2.1 Experimental setup

In the SMI, the common setup is based on the use of built-in monitor photodetector. When not available, one needs to setup with an external photodetector. In this case, using an external photodetector gives us an opportunity to choose suitable properties such as the bandwidth and quantum efficiencies. Moreover, it is shown that using a balanced detection setup with an external and internal photodetector gives an improved signal-to-noise ratio and enhanced self-mixing signal [13].

In the experiment, commercial laser diode of 808 nm (LD-808-100A, Thorlabs) was positioned 30 cm away from the target and the current and temperature of laser diode was controlled by the ITC-4005, Thorlabs. The collimated laser beam emitted by the laser diode is directed toward the accelerometer after passing through the neutral density (ND) filter. The ND filter functions as both beam splitter and feedback controller. Beam splitter splits the beam into two orthogonal directions of which one goes to the detector and the other goes to the target. Because it is continuously variable, amount of optical feedback can be controlled by moving it manually on its micro stage to the region where it is darker or lighter. The optimum position is decided by tracing and observing the self-mixing signal. Accelerometer (triaxial ICP accelerometer, model

Table 1: Comparison of previous and current work

Previous work	Contribution	Our contribution
Usman Zabit *et al.* [10,12]	Parasitic vibrations have been eliminated by using a self-mixing displacement sensor that senses the parasitic vibrations transmitted to the SM sensor by using a solid state accelerometer based on a microelectromechanical system	Self-mixing interferometer with ceramic shear-based piezoelectric accelerometer with the SMI has been used
Bernal *et al.* [13]	The inherent error as well as the robustness of a previously published displacement retrieval technique called the PUM is analyzed. This analysis, based on a detailed study of laser feedback phase behavior, results in a new algorithm that removes the PUM inherent error while maintaining its robustness	PUM has been applied with ceramic accelerometer which has better resolution than most of the solid state type accelerometers

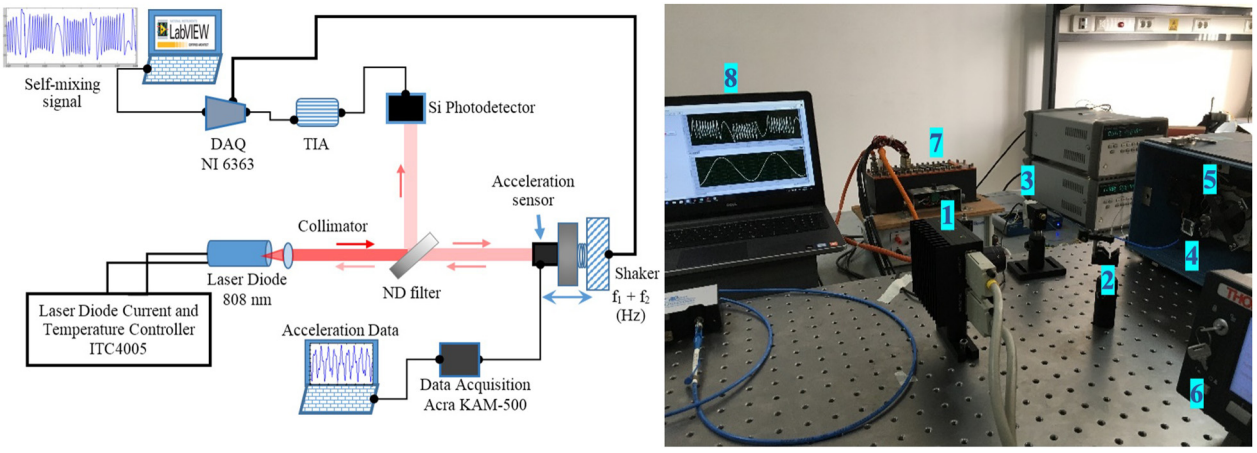

Figure 1: The experimental setup of the semiconductor SMI with an external photodiode. On the right figure, numbers from 1 to 8 correspond to the laser diode, the ND filter, Si photodiode, accelerometer, shaker, ITC-4005, ACRA KAM-500 data acquisition system for accelerometer, and notebook for LabVIEW control, respectively.

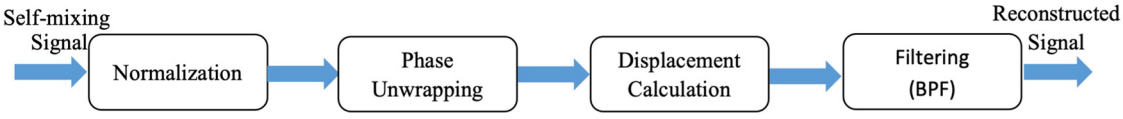

Figure 2: Schematic block diagram of PUM applied to the self-mixing signal for the reconstructed displacements.

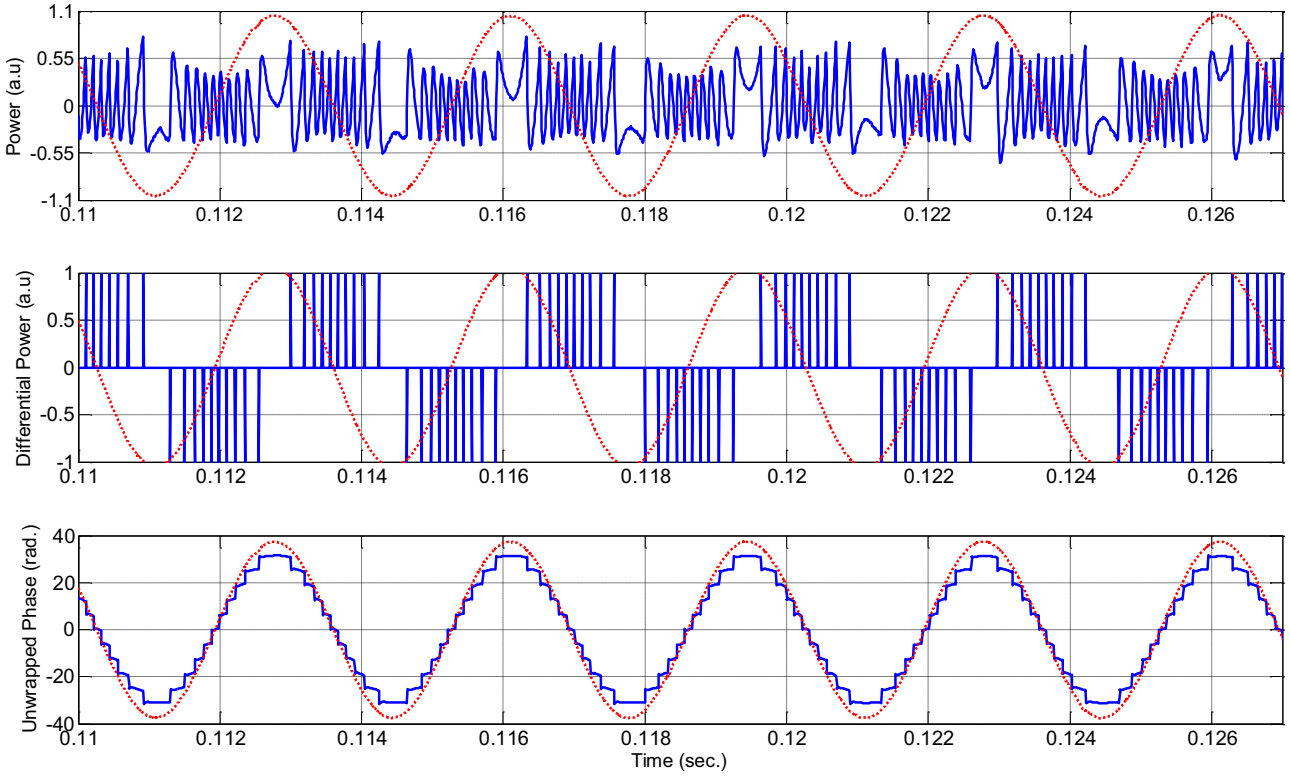

Figure 3: Case 1: 300 Hz, 35 mV sinusoidal signal. From top to down: self-mixing signal, differentiation of power, and unwrapped phase. Red dotted curve represents the target motion generated by the NI-6363 and their values were scaled to the graphs.

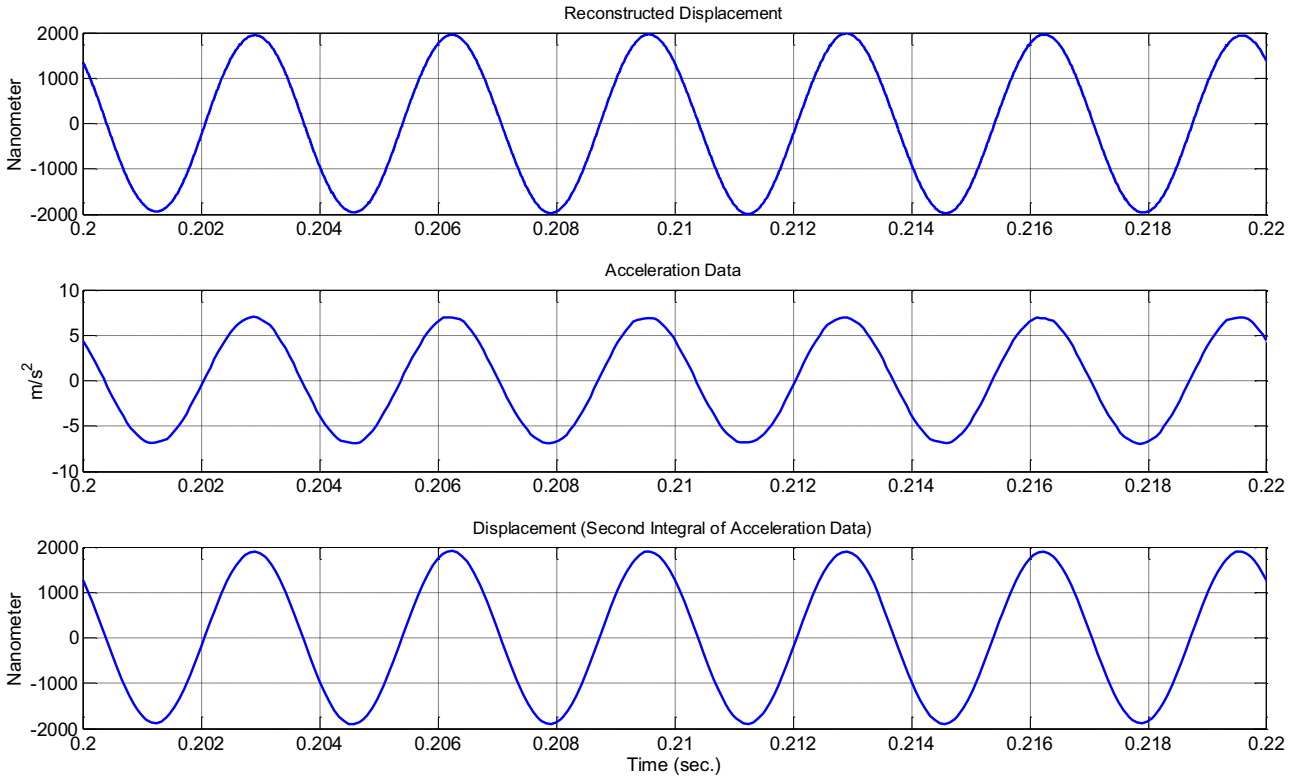

Figure 4: Case 1: 300 Hz, 35 mV sinusoidal signal. From top to down: reconstructed displacement using the phase unwrapped algorithm, acceleration data, and second integral of acceleration.

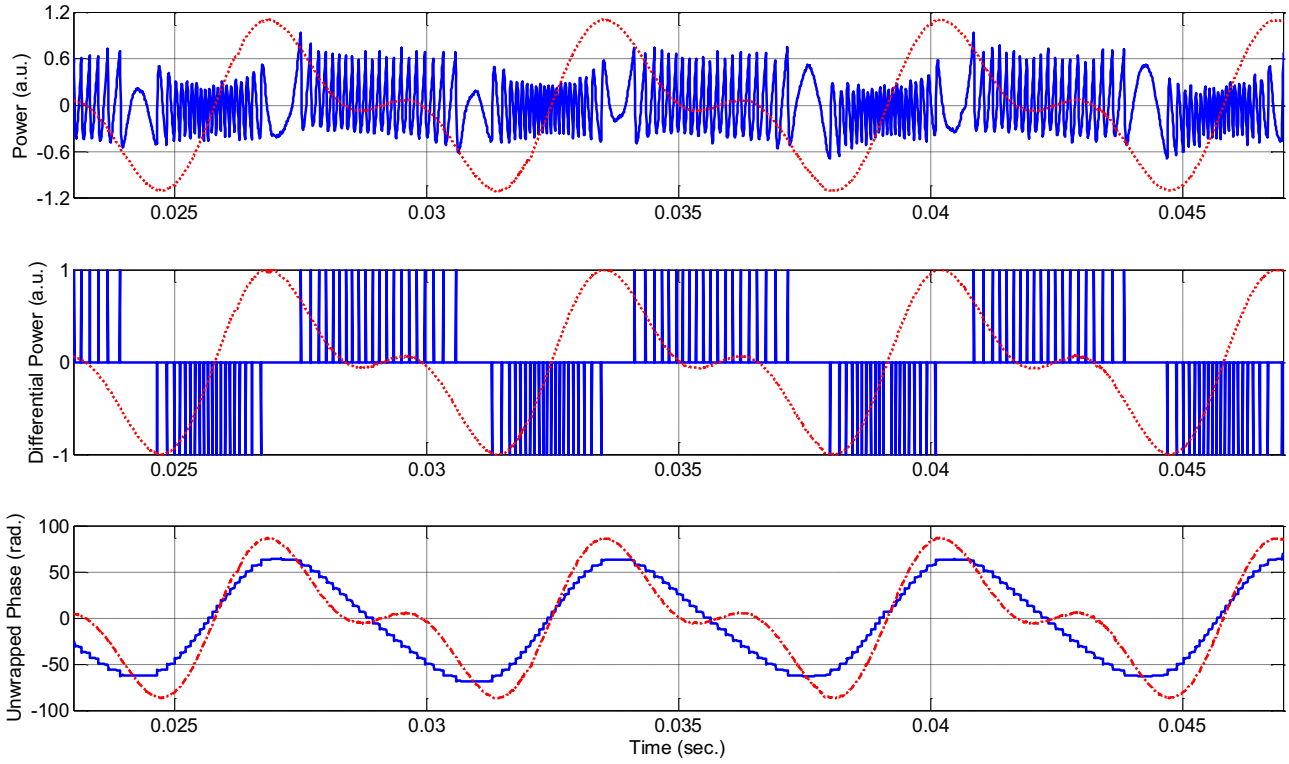

Figure 5: Case 2: sum of 150 Hz, 15 mV and 300 Hz, 10 mV. From top to down: self-mixing signal, differentiation of power, and unwrapped phase. Red dotted curve represents the target motion generated by the NI-6363 and their values were scaled to the graphs.

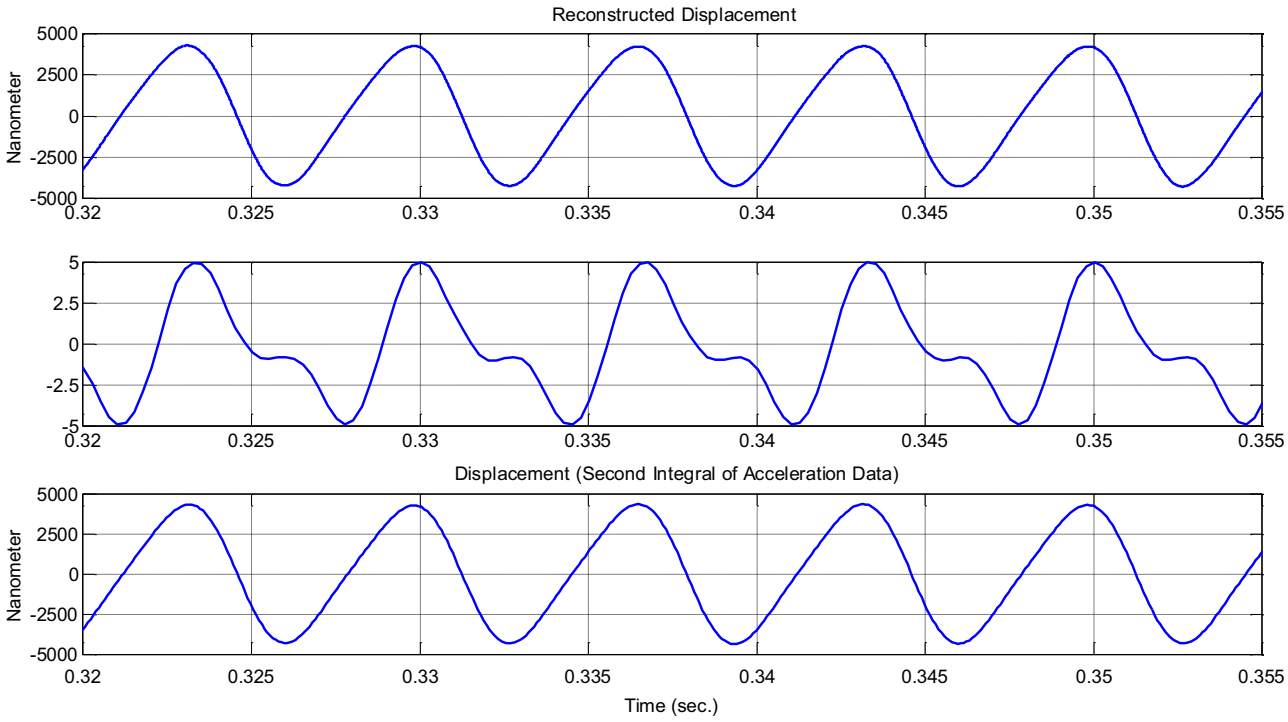

Figure 6: Case 2: sum of 150 Hz, 15 mV and 300 Hz, 10 mV. From top to down: reconstructed displacement using the phase unwrapped algorithm, acceleration data, and second integral of acceleration. The acceleration data in the middle were acquired by the piezoelectric (ceramic shear) based accelerometer.

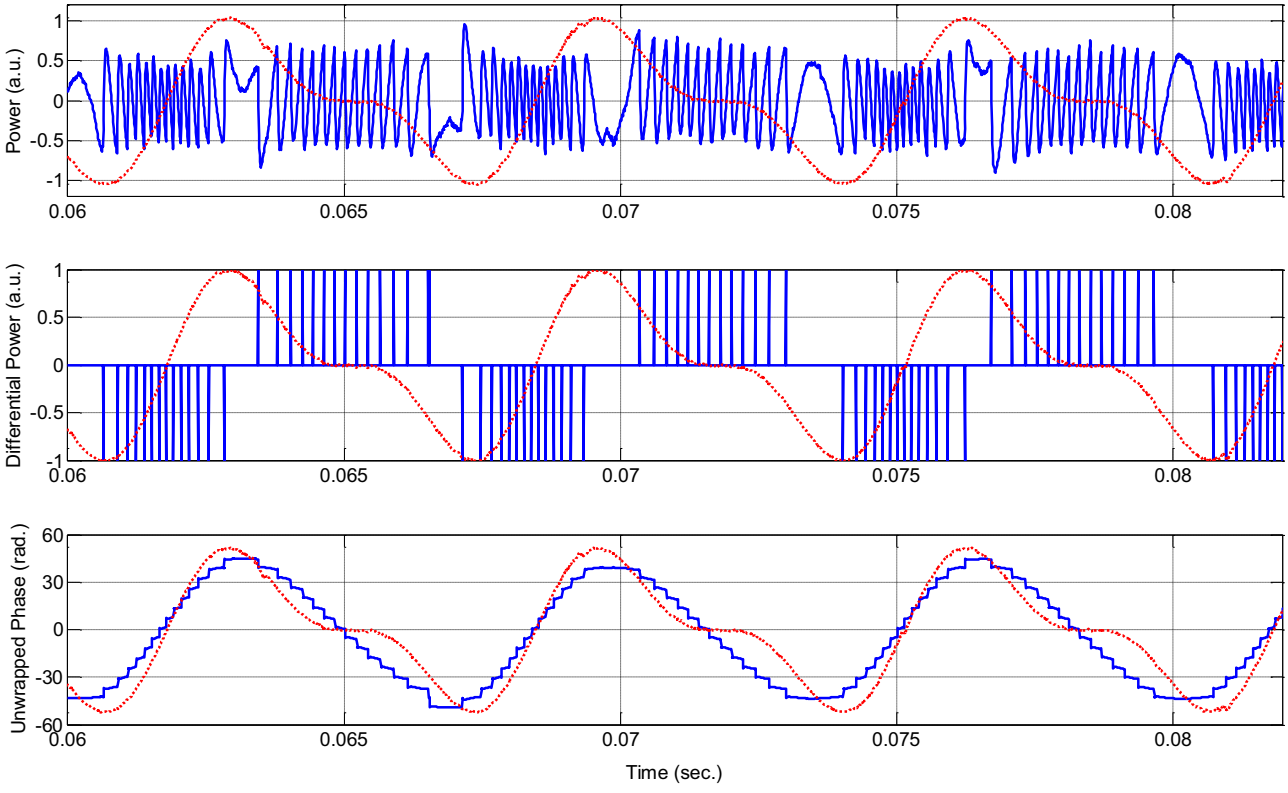

Figure 7: Case 3: sum of 150 Hz, 10 mV and 300 Hz, 5 mV. From top to down: self-mixing signal, differentiation of power, and unwrapped phase. Red dotted curve represents the target motion generated by the NI-6363 and their values were scaled to the graphs.

Table 2: Comparisons of all three cases

Sine driven oscillation	Reconstructed displacement (nm)	Integral displacement (nm)	Difference between wavelengths (nm)	Raw accelerometer value (m/s^2)	Displacement formula result (Eqs. [3] and [4]) (nm)
300 Hz, 35 mV	3,870 ± 35	3,805 ± 45	65 ± 30	14.06 ± 0.12	3,900 ± 25
150 Hz, 15 mV + 300 Hz, 10 mV	8,550 ± 35	8,615 ± 25	65 ± 20	10.56 ± 0.07	8,466 ± 50
150 Hz, 10 mV + 300 Hz, 5 mV	5,660 ± 30	5,650 ± 20	10 ± 15	6.56 ± 0.06	5,652 ± 48

no. 356A16, PCB Piezotronics) was attached to the shaker firmly that is controlled by the computer *via* Acra KAM-500 Data Acquisition Systems. Spectral noise performance of the accelerometer at 300 Hz is given as 3 $\mu g/Hz^{1/2}$, its sensitivity is given as 100 mV/g and its broadband (1–10,000 Hz) resolution is 0.0001 g (RMS), where g is the acceleration due to gravitational force. SMI signal was collected by the data acquisition module (NI, USB-6363) and the shaker was driven with the same module at the desired frequencies. The optical feedback was controlled by simply moving the ND filter manually which changes the optical power along the optical path. The calibration of accelerometer was checked by the calibration exciter (Type 4294, Brüel&Kjaer) that drives the accelerometer with oscillation of angular frequency of w = 1,000 rad/s which corresponds to 10 m/s^2 (RMS) acceleration. Figure 1 shows our optical setup with drawing and the real pictures.

For all experiments, the acceleration data whose sampling frequency was set to 4 kHz was acquired by another computer. We could not obtain the SMI signal and the acceleration data simultaneously because of hardware difficulty of the accelerometer. Accelerometer has its own old-fashioned data acquisition system which is impossible to integrate it to our LabVIEW environment for self-mixing. But the figures are plotted as they are synchronized. However, we obtained synchronously the self-mixing signal and sinusoidal signal that drive the shaker and are all controlled by the NI DAQ card.

For the reconstructed displacement from the self-mixing signal, PUM has been used to extract the phase from $P_f(t)$ that allows displacements with a resolution of almost $\lambda/20$ [14]. Figure 2 shows the block diagram of the reconstruction method implemented in Matlab.

3 Results and discussion

In the first case, the shaker was driven with a 300 Hz and 35 mV sinusoidal oscillation. For this single frequency oscillation, in order to find the displacement, we can make use of the accelerometer data that gives peak-to-peak $a_{pp} = (1.43 \pm 0.01) \times g$ m/s^2 where g is taken to be 9.81 m/s^2. Then, we can find the peak-to-peak displacement by using the following formula,

$$x_{pp} = \frac{a_{pp}}{(2 \times \pi \times f)^2}, \tag{3}$$

where f is 300 Hz. This gives approximately 3,900 ± 25 nm. When sum of two frequencies are given to the shaker, then Eq. (3) becomes

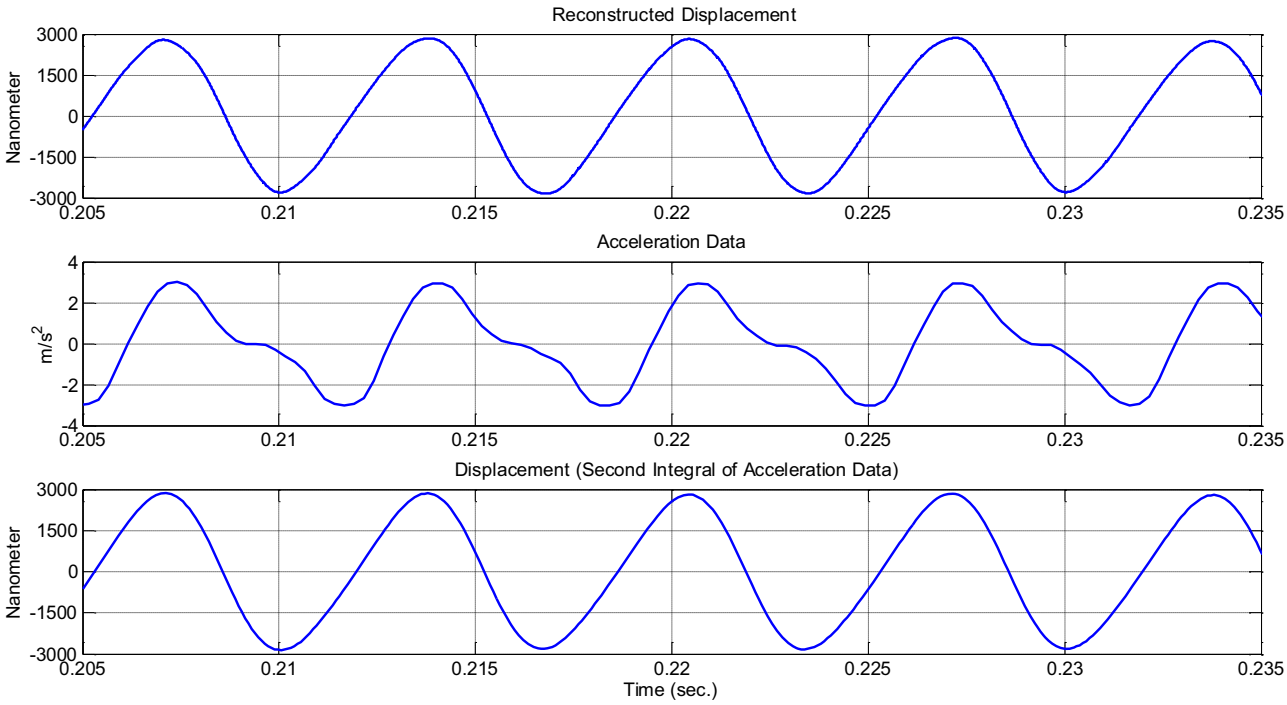

Figure 8: Case 3: sum of 150 Hz, 10 mV and 300 Hz, 5 mV. From top to down: reconstructed displacement using the phase unwrapped algorithm, acceleration data, and second integral of acceleration. The acceleration data in the middle were acquired by the piezoelectric (ceramic shear) based accelerometer.

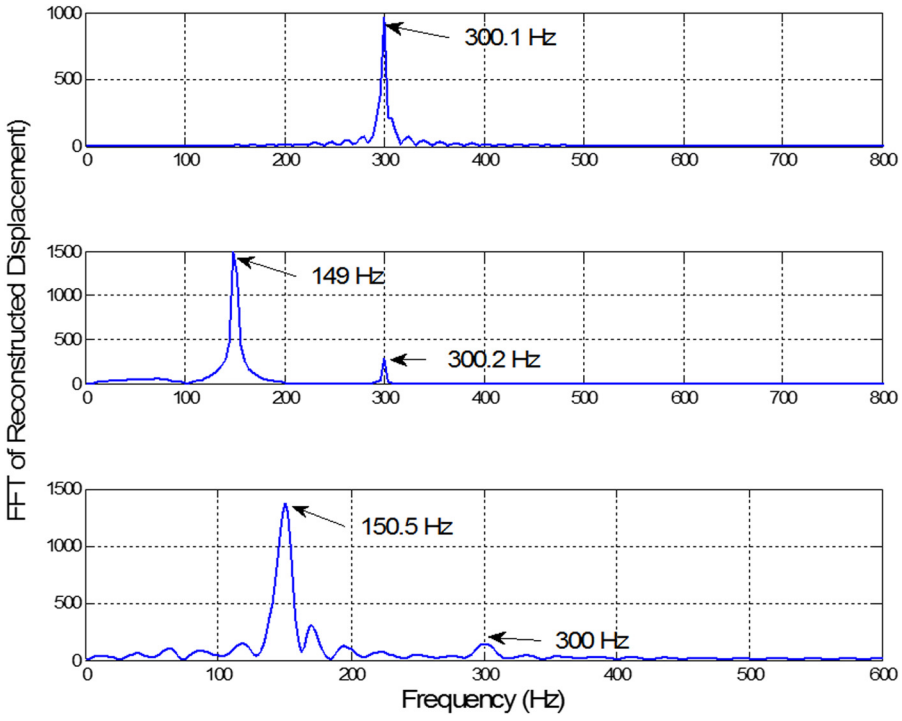

Figure 9: Fast fourier transform (FFT) results of constructed displacements for three cases.

$$x_{pp} = \frac{a_{pp}}{(2 \times \pi \times f_1)^2} + \frac{a'_{pp}}{(2 \times \pi \times f_2)^2}. \quad (4)$$

Self-mixing signal and phase unwrapping of the first case is shown in Figure 3. As can be seen, self-mixing signal resembles saw-tooth, so the C-parameter can be expected to be between 1 and 2. The red dotted curve represents the target motion under the driving frequency (Hz) and amplitude (mV). It was added to the graphs just to see the motion of target and their values are scaled to the graphs.

Top and bottom of Figure 4 are the reconstructed displacements and the second integral of the middle data which is the acceleration data. As seen, the motion is exactly sinusoidal with a driven frequency of 300 Hz. Similar graphs are plotted for the second and third cases which are sum of 150 Hz, 10 mV and 300 Hz, 5 mV, and the sum of 150 Hz, 15 mV and 300 Hz, 10 mV, respectively.

Figures 5–8 are the second and third cases, where we drive the target with two different frequencies and amplitudes. Self-mixing signal changes from the first case as the self-mixing signal is denser at rising edge of the driving signal than that of falling edges which can be clearly seen at the top of Figures 5 and 7.

In order to get the displacement from the accelerometer data, we just integrate twice by using trapezoid rule. Before and after the first integral, we have chosen the Butterworth filter in Matlab since it is maximally flat with minimal ripple. This filtering must be applied otherwise integral constant becomes time dependent after the second integral and this gives erroneous result.

All these figures present very good results as summarized in Table 2. If we take the theoretical result as references (last column in the table) which was obtained by the peak-to-peak fluctuation of the raw accelerometer data, reconstructed displacements from both self-mixing and accelerometer signal are very close to the theoretical results. By taking the FFT of the reconstructed displacements from the self-mixing signal, we get Figure 9, which shows good agreement with driven the oscillation frequencies. The signal at 150 Hz appears to be more dominant than that at 300 Hz because of its higher driven amplitude.

4 Conclusion

In summary, we make a comparative study to obtain displacements of vibrating target by using two different ways, one of which is with ceramic-based piezoelectric accelerometer as a reference and the other is SMI. Butterworth filtering technique must be used to get correct displacement from the raw accelerometer data. Self-mixing interferometric method has given very good results with a proximity of 10, 30, and 90 nm results when compared to the theoretical results. Differences between the two methods are also in good agreement to each other which are 65 and 10 nm. When the error in the data is considered, differences can go up to approximately 100 nm at most.

Acknowledgements: The authors gratefully thank Prof. Dr Reşat Ozgur Doruk for guidance through preparation.

Funding information: This work was financially supported by Ankara Haci Bayram Veli University Scientific Research Project (Project Number: 01/2021-05) and Gazi University Scientific Research Project (Project Number: 18/2015-03).

Author contributions: All authors have accepted responsibility for the entire content of this manuscript and approved its submission.

Conflict of interest: The authors state no conflict of interest.

References

[1] Giuliani G, Norgia M, Donati S, Bosch T. Laser diode self-mixing technique for sensing applications. J Opt A Pure Appl Opt. 2002;4:283–94. doi: 10.1088/1464-4258/4/6/371.

[2] Tambosso T, Horng RH, Donati S. Curvature of substrates is measured by means of a self-mixing scheme. IEEE Photonics Technol Lett. 2014;26:2170–2. doi: 10.1109/LPT.2014.2349958.

[3] Reza Atashkhooei EER, Miquet RC, Moreira A, Quotb S, Royo J. Perchoux, optical feedback flowmetry: impact of particle concentration on the signal processing method. IEEE Sens J. 2018;18:4.

[4] Donati S, Martini G, Hwang S-K. Measurement of ambient vibration by self-mixing interferometry and its application to intrusion detection. Opt Eng. 2018;57(5):051508.

[5] Candan C, Tiken M, Orhan E, Berberoglu H. Determination of balance degree of spinning gyro disk by using optical feedback interferometry. Proc. SPIE 10695, optical instrument science, technology, and applications. Frankfurt, Germany: SPIE European Optical Design Conference; 2018. p. 106950X.

[6] Wang WM, Boyle WJO, Grattan KTV, Palmer AW. Self-mixing interference in a diode laser: experimental observations and theoretical analysis. Appl Opt. 1993;32:1551. doi: 10.1364/AO.32.001551.

[7] Li K, Cavedo F, Pesatori A, Zhao C, Norgia M. Balanced detection for self-mixing interferometry. Optics Letters. 2017;42(2):283–5. doi: 10.1364/OL.42.000283.

[8] Bes C, Plantier G, Bosch T. Displacement measurements using a self-mixing laser diode under moderate feedback. IEEE Trans Instrum Meas. 2006;55:1101–5. doi: 10.1109/TIM.2006.876544.

[9] Lang R, Kobayashi K. External optical feedback effects on semiconductor injection laser properties. IEEE J Quantum Electron. 1980;16:347–55. doi: 10.1109/JQE.1980.1070479.
[10] Zabit U, Bernal OD, Bosch T, Bony F. MEMS accelerometer embedded in a self-mixing displacement sensor for parasitic vibration compensation. Optics Letters. 2011;36(5):612–4.
[11] Wang WM, Grattan KTV, Palmer AW, Boyle WJO. Self-mixing interference inside a single-mode diode laser for optical sensing applications. J Light Technol. 1994;12:1577–87. doi: 10.1109/50.320940.
[12] Zabit U, Bosch T, Bony F. Adaptive transition detection algorithm for a self-mixing displacement sensor. IEEE Sens J. 2009;9:1879–86. doi: 10.1109/JSEN.2009.2031496.
[13] Bernal OD, Zabit U, Bosch T. Study of laser feedback phase under self-mixing leading to improved phase unwrapping for vibration sensing. IEEE Sens J. 2013;13:4962–71. doi: 10.1109/JSEN.2013.2276106.
[14] Donati S. Developing self-mixing interferometry for instrumentation and measurements. Laser Photonics Rev. 2012;6:393–417. doi: 10.1002/lpor.201100002.